Inferring a novel insecticide resistance metric and exposure variability in mosquito bioassays across Africa

Adrian Denz[1,2], Mara D. Kont[3], Antoine Sanou[4,5], Thomas S. Churcher[3], Ben Lambert[6,7]

1 School of Mathematical Sciences, University of Nottingham, Nottingham, UK (previous institution)
2 Faculty of Economics, Università della Svizzera italiana, Lugano, Switzerland (current institution)
3 MRC Centre for Global Infectious Disease Analysis, Department of Infectious Disease Epidemiology, Imperial College London, UK
4 Centre National de Recherche et de Formation sur le Paludisme, Ouagadougou, Burkina Faso
5 Institut Supérieur du Développement Durable, Université de Fada N'Gourma, Burkina Faso
6 Department of Statistics, University of Oxford, Oxford, UK
7 Pandemic Sciences Institute, University of Oxford, Oxford, UK

Abstract

Malaria claims approximately 500,000 lives each year, and insecticide-treated nets (ITNs), which kill mosquitoes that transmit the disease, remain the most effective intervention. However, resistance to pyrethroids, the primary insecticide class used in ITNs, has risen dramatically in Africa, making it difficult to assess the current public health impact of pyrethroid-ITNs. Past work has modelled the relation between pyrethroid susceptibility measured in discriminating-dose susceptibility bioassays and ITN effectiveness in experimental hut trials. Here, we introduce a new predictive approach that accounts for heterogeneity in insecticide resistance within wild mosquito populations, for example, due to genetic variability, by incorporating data from newly recommended intensity-dose susceptibility bioassays. We fit our mathematical model to a comprehensive data set that combines discriminating dose bioassays from all over Africa, intensity dose bioassays from Burkina Faso, and concurrent experimental hut trials. Our analysis estimates location- and insecticide-specific variation in resistance heterogeneity in Burkina Faso and quantifies differences in insecticide exposure in bioassays and experimental huts. By providing a mechanistic understanding of these experimental data, our approach could be integrated into malaria transmission models to account for the public health impact of insecticide resistance detected by surveillance programmes.

Introduction

Malaria kills more than half a million people worldwide each year [1] and is transmitted by mosquitoes of the Genus *Anopheles*. Insecticide treated bednets (ITNs) protect individuals sleeping under them from blood-feeding mosquitoes but more importantly kill mosquitoes, which provides a community-level protection against disease [2–7].

From 2000 until the mid-2010s, the number of deaths from malaria fell dramatically, primarily due to the widespread use of ITNs [8]. However, the emerging resistance in mosquitoes to the pyrethroid insecticides used in ITN formulations has led to a debate about the continued effectiveness of ITNs [9–16]. Large trials were conducted to assess the impact of resistance to pyrethroids on the effectiveness of ITN-based malaria vector control [17, 18], but quantifying the impact of resistance by comparison across epidemiological settings is difficult due to many interfering factors [19] and so the overall impact of mosquito resistance threat remains unclear [20].

In addition to quantifying the malaria burden due to loss of ITN effectiveness through the spread of pyrethroid resistance, it is important to factor in resistance in localised malaria prevention planning. Simulation models of malaria epidemiology [21–23] take into account many epidemiological factors and are increasingly used for the fine-scale planning of intervention strategies. These models require parameterising the differential effects on malaria transmission for each ITN product taking into account insecticide resistance in mosquitoes. In particular, decisions about what ITN product to use in a specific setting depend on its ability to kill mosquitoes with different resistance profiles [24].

Experimental hut trials (EHT) are a standard assay to evaluate ITN products under controlled field conditions [25] and are the primary data source for parameterising their entomological impact in models of malaria epidemiology [13, 26–28]. An experimental hut mimics typical housing in the study area but is specially constructed to retain all entering mosquitoes, with three main hut designs used in Sub-Saharan Africa: East African [29], West African [30] and Ifakara design [31]; which differ in catching efficiency [32]. During an EHT, a human volunteer sleeps inside the hut under either an untreated control net or an ITN, and after each study night, all dead and alive mosquitoes are collected from the hut and their blood-feeding status recorded. From these detailed data, ITN effects on mosquito survival and blood-feeding can be estimated [13, 26–28]. EHTs are relatively laborious and expensive, and so are conducted in a limited number of locations only.

Programmes to monitor pyrethroid resistance occurrence across Sub-Saharan Africa were established and have captured large amounts of data [33, 34]. There are two main susceptibility bioassays (SB) used for pyrethroid resistance surveillance: the World Health Organisation (WHO) tube protocol [35] and the U.S. Centers for Disease Control and Prevention (CDC) bottle protocol [36]. Under either protocol, offspring of wild mosquitoes are exposed to insecticidal material of a standardised concentration inside a small container for a given amount of time, and the count of dead mosquitoes is recorded. When testing pyrethroid insecticides with the WHO tube protocol, the expose time is 1 hour and a 24 hour post-exposure holding period is applied before mortality assessment. Mosquito samples are obtained by collecting larvae or blood-fed mothers from the field and rearing under standardised conditions. SBs were designed to detect the emergence of resistance in a mosquito population [18, 35] and do not aim to directly capture the impact of resistance on ITN efficacy. The most widely used SB is the discriminating dose bioassay (DD-SB), which operates with a single dose of insecticide to discriminate between fully susceptible and potentially resistant mosquito populations. That discriminating dose, however, does not relate to the insecticide exposure upon interaction with an ITN in the field [13]. Nevertheless, statistical models extrapolating DD-SB data were used to predict the impact of pyrethroid resistance on ITN effectiveness in experimental hut trials [13, 28], and this parameterisation included within transmission dynamics models was broadly able to predict the results of cluster randomised control trials of the mass deployment of different ITNs [37].

In order to better quantify pyrethroid resistance in a mosquito population, intensity-dose bioassays (ID-SB), which assess mosquito susceptibility for a range of

insecticide doses, were developed [35,38] and are increasingly used [39]. A first framework for their analysis proposed fitting a generalised logistic function to ID-SB data and deriving the distribution of lethal doses in the population, from which the lethal dose with respect to any mortality level can be determined [40]. However, these models are non-mechanistic, potentially limiting their practical use for characterising the impact of pyrethroid resistance on disease transmission. In addition, currently no method is available to integrate data from DD-SB and ID-SB to predict the effectiveness of ITNs.

We propose a simple, mechanistic model of insecticide-induced mortality in mosquito bioassays that incorporates stochasticity in insecticide exposure and tolerance to insecticide. Our model allows us to characterise ID-SB data by two parameters: the median lethal dose (LD_{50}), at which half of mosquitoes are killed, and the standard deviation of the logarithm of the lethal dose as a measure of the heterogeneity in insecticide tolerance. To date, resistance to pyrethroids in a mosquito population is typically characterised by a single value, the fraction of mosquitoes dying, and the heterogeneity of resistance in the population is largely overlooked [9]. While purely statistical models of ID-SB data impose essentially arbitrary functional relationships, the proposed model requires only distributional assumptions on insecticide exposure and tolerance. More generally, it provides a unified treatment of SBs, which are the standard for pyrethroid resistance monitoring, and EHTs, which present a more realistic model system of how mosquitoes interact with insecticides in the field. By fitting our model to the matched SB and EHT data, we obtain a predictive model of the effectiveness of ITN given the SB data.

Materials and methods

Data

Following our objective of predicting EHT outcomes from SB data, we only use data from EHT studies where the level of insecticide resistance in the local mosquito population had been characterised in SBs. Both the SB and EHT studies report counts of the number of female *Anopheles* mosquitoes dying, see Fig 1 for a graphical summary. We extended an existing data set of matched DD-SB and EHT studies [28] with a recent study from Burkina Faso comprising EHT and ID-SB data. We included only SB studies on wild-type mosquitoes exposed to single pyrethroid insecticides. All SB studies followed the WHO tube protocol [35], except for one which used a comparable protocol conducted before 2000. We considered only EHT data on single active ingredient, pyrethroid ITNs that were new and unwashed. ITN products which use the same insecticide, but which may differ in other characteristics, were treated the same in our analysis. For the EHT data, we pooled the number of mosquitoes collected across all hut compartments considered in the corresponding study, and mortality counts were determined after a 24-hour recovery period. We did not consider the hut or sleeper volunteer identity as covariates given that previous work indicated that these variables only account for a minor portion of the variation in mosquito mortality across observations [41]. Stratification of mosquito counts by species was not consistent between studies, so for both SB and EHT data, we pooled data for all reported *Anopheles* species. An SB and an EHT study were considered a match if they were conducted in the same village-sized geographical location and in the same year. Within each match, the data were further grouped by insecticide if the insecticides present as active ingredients of the ITNs trialled in the EHT study were all tested in the SB study. If for none of the ITNs the active ingredient was tested in the matched SB study, the data on all the pyrethroid insecticides tested in the SB were pooled, i.e. studies that

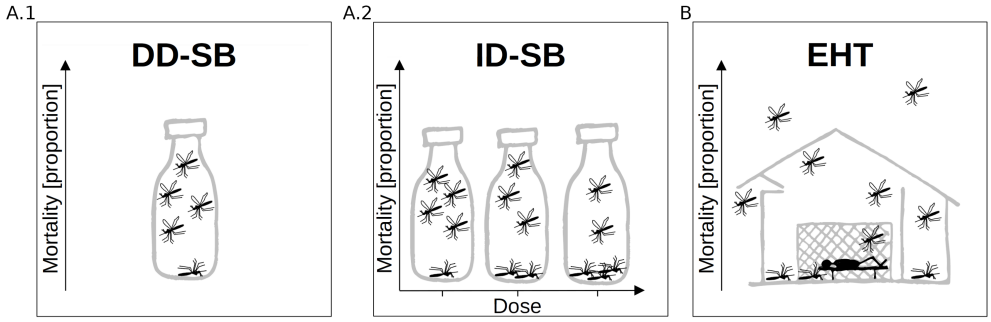

Fig 1. Insecticide bioassay types. A.1 Discriminating-dose susceptibility bioassay (DD-SB) and **A.2** intensity-dose susceptibility bioassay (ID-SB), both depicted by the CDC bottle bioassay. **B** Experimental hut trial (EHT), depicted by the East African hut type.

used different types of pyrethroid were still matched, making the assumption that there is cross resistance within the pyrethroid class [42]. This procedure led to a total of 35 assay pairs of matched SB and EHT data. Control SBs (without insecticide) and EHT control arms (using untreated nets) were included and shared among assay pairs from the same study, without replicating any data. The characteristics and sample sizes per assay pair are listed in Table 1, including references to the original studies. Overall, the data set we used to fit the model includes data for 18,623 mosquitoes observed in SB studies and 110,054 mosquitoes observed in EHT studies (see Table 1 and S1 Table for a summary of all data used).

Table 1. Summary of paired ID-SB and EHT data from Burkina Faso used in this study.

Assay pair	Site	Year	Insecticides in SB	Insecticides on ITNs	ITN products	Total in treatment SB	Total in control SB	Total in intervention hut	Total in control hut
1	Tengrela	2020	alphacypermethrin	alphacypermethrin	Interceptor	1214	997	283	731
2	Tengrela	2021	alphacypermethrin	alphacypermethrin	Interceptor	804	612	802	886
3	Tiefora	2020	alphacypermethrin	alphacypermethrin	Interceptor	1721	1376	228	627
4	Tiefora	2021	alphacypermethrin	alphacypermethrin	Interceptor	960	929	213	321
5	Tengrela	2019	deltamethrin	deltamethrin	PermaNet2	387	318	546	830
6	Tengrela	2020	deltamethrin	deltamethrin	PermaNet2	1353	997	774	731
7	Tiefora	2020	deltamethrin	deltamethrin	PermaNet2	1673	1376	452	627

All data are from Burkina Faso [43]. Intensity-dose susceptibility bioassays (ID-SB) were conducted according to the WHO tube protocol [35] and experimental hut trials (EHT) used the West African experimental hut design [30]. Note that controls may be shared across assay pairs. For a summary of the paired discriminating-dose susceptibility bioassay (DD-SB) and EHT data additionally used in this study see S1 Table.

Mechanistic model for insecticide-induced mosquito mortality

Previous models exploring the relationship between insecticide-induced mosquito mortality in the different assays have assumed that all mosquitoes in a DD-SB have the same probability of dying [13, 28]. For ID-SBs, previous work has allowed for heterogeneity in the lethal dose within a mosquito sample, but assumed a uniform exposure to the insecticide [40]. Here we propose a mechanistic model which allows both the insecticide exposure and the maximal insecticide tolerance (measured on 'Dose' scale and referred to as the 'Lethal dose') to vary between individual mosquitoes by treating those quantities as random variables. Given distributional assumptions, the probability that a mosquito dies depends on assay-specific parameters of the exposure distribution and on the parameters of the lethal dose distribution, which collectively characterise the level of resistance of the corresponding entomological setting. Empirical

evidence supports the assumption of heterogeneity in both insecticide exposure and tolerance. For example, variability in insecticide exposure has been observed in confined spaces using video cone tests [44] or in EHT setups using room-scale video tracking [45]. Conversely, a wide section of genetic markers have been associated with pyrethroid-resistant phenotypes in wild mosquitoes [46], and polygenic resistance phenotypes [47] likely exhibit variability in lethal dose. In the absence of data to estimate the correlation between exposure and lethal dose in individual mosquitoes, we make the parsimonious assumption that exposure and lethal dose are independent of each other, while the model would allow for inclusion of a correlation coefficient. The heterogeneity of the exposure varies between bioassays and EHTs, and we assume that the tolerance of mosquitoes from the same population is the same in both assays. A summary of all model parameters is given in Table 2.

Mortality in susceptibility bioassays

Mosquitoes in a SB are heterogeneously exposed to the insecticide due to variation in individual behaviour and we model the exposure heterogeneity stochastically. Let the insecticide exposure of an individual mosquito i in a SB be a positive random variable, X_i, with a measuring unit 'insecticide mass'. We assume $X_i = V_i c$, where V_i is a positive random variable representing the volume of insecticidal material mosquito i comes into contact with and c is the average insecticide concentration in a unit volume. Note that we use the term volume in a broad sense, including all uptake of insecticidal material during the bioassay, such as through surface contact with the insecticide carrier and through contact with vaporised insecticide in the air. We further assume that the concentration c is a linear function $c = \alpha d$ of the dose d of insecticide applied to the carrier in the SB, with the dose d measured as multiples of the discriminating dose defined by the WHO [35]. We model V_i as log-normally distributed to account for the likely large variability in mosquito exposure to insecticide in the SB. By appropriately rescaling the volume measuring unit – corresponding to e.g. switching from inches^3 to centimeters^3 – we can assume $\log(V_i)$ has mean $-\log(\alpha)$ without loss of generality. Hence, the exposure $X_i = \alpha d V_i$ follows a log-normal distribution and due to the rescaling α vanishes from the equation:

$$\log(X_i) \sim \mathcal{N}(\log(d), \sigma_{\mathrm{SB}}), \tag{1}$$

where $\sigma_{\mathrm{SB}} > 0$. The measurement unit for exposure is 'insecticide mass' but due to the change in the volume scale, it has the same scale as 'Dose', measured as multiples of the discriminating dose defined by the WHO [35].

We represent the lethal dose for mosquito i as a positive random variable T_i and assume that mosquito i dies in the 24 hours post exposure (the holding time of mosquitoes in both SB and EHT for insecticides with a fast mode of action, such as the pyrethroid products considered here) if $X_i > T_i$. The indicator random variable for death due to the insecticide $\mathbf{1}_{X_i > T_i}$ has a Bernoulli distribution with probability

$$p^{(1)}{}_{\mathrm{SB}} = \mathbb{P}(X_i > T_i). \tag{2}$$

However, mosquitoes can also die due to other exogenous factors during the holding time of the assay, and we assume an additional independent Bernoulli death process with probability $p^{(0)}{}_{\mathrm{SB}}$. By the law of total probability, the death of mosquito i is a Bernoulli random variable with probability

$$p_{\mathrm{SB}} = p^{(0)}{}_{\mathrm{SB}} + \left(1 - p^{(0)}{}_{\mathrm{SB}}\right) p^{(1)}{}_{\mathrm{SB}}. \tag{3}$$

Mortality in susceptibility bioassays for field-collected mosquitoes

Mosquitoes sampled from a wild population exhibit variable insecticide susceptibility, due to genetic variation and variation in environmental conditions during both juvenile and adult life stages. We assume that the lethal dose T_i for an individual mosquito i is independent of its exposure X_i and is distributed following a log-normal distribution

$$\log(T_i) \sim \mathcal{N}(\mu_{\mathrm{T}}, \sigma_{\mathrm{T}}), \tag{4}$$

where the mean μ_{T} and the standard deviation σ_{T} characterise the lethal dose distribution within a given population. By the monotonicity of the log function and the symmetry of the standard normal distribution, the probability of insecticide-induced death can be computed as

$$\begin{aligned} {p^{(1)}}_{\mathrm{SB}} &= \mathbb{P}(X_i > T_i) \\ &= \mathbb{P}\left(\log(T_i) - \log(X_i) < 0\right) \\ &= \mathbb{P}\left(\log(T_i) - \log(X_i) - (\mu_{\mathrm{T}} - \log(d)) < \log(d) - \mu_{\mathrm{T}}\right) \\ &= \Phi\left(\frac{\log(d) - \mu_{\mathrm{T}}}{\sqrt{\sigma_{\mathrm{SB}}^2 + \sigma_{\mathrm{T}}^2}}\right), \end{aligned} \tag{5}$$

where Φ denotes the cumulative distribution function of the standard normal. To derive Eq. 5, we used the fact that the sum of two independent normal distributed random variables is normally distributed with mean equal to the sum of the two means and variance equal to the sum of the variances. For an illustration of Eq. 5 see Fig 2.

From Eq. 5 it follows that LD_{50}, the dose at which 50% of the mosquitoes die, is given by $\exp(\mu_{\mathrm{T}})$ in our model, the median of T_i. This is due to the symmetry of the exposure and lethal dose distributions on the logarithmic scale and the monotonicity of the logarithm. The parameters σ_{T} and σ_{SB} define the shape of the dose-response curve; see Fig 3 for a an illustration. This model allows us to characterise the insecticide resistance of a mosquito population by location and scale parameters: the median lethal dose ($\exp(\mu_{\mathrm{T}})$), and the standard deviation of the logarithm of the lethal dose (σ_{T}) as a measure of the heterogeneity in insecticide tolerance.

Mortality in experimental hut trials

For EHTs we use a similar model. We assume that mosquitoes from the local population enter the experimental hut randomly and independently of their individual lethal dose. Note that this means that we assume that there is no behavioural resistance to the insecticide, and that each mosquito entering the hut has a lethal dose T_i distributed as in Eq. 4 with parameters μ_{T} and σ_{T} corresponding to the local population. We then assume that each mosquito i in the hut experiences an exposure X_i that is independent of its lethal dose T_i and distributed according to

$$\log(X_i) \sim \mathcal{N}(\mu_{\mathrm{EHT}}, \sigma_{\mathrm{EHT}}), \tag{6}$$

with parameters μ_{EHT} and $\sigma_{\mathrm{EHT}} > 0$. Like in SBs, we assume that a mosquito i dies if $X_i > T_i$ and by Eq. 2 the probability of death due to insecticide is

$$\begin{aligned} {p^{(1)}}_{\mathrm{EHT}} &= \mathbb{P}(X_i > T_i) \\ &= \Phi\left(\frac{\mu_{\mathrm{EHT}} - \mu_{\mathrm{T}}}{\sqrt{\sigma_{\mathrm{EHT}}^2 + \sigma_{\mathrm{T}}^2}}\right). \end{aligned} \tag{7}$$

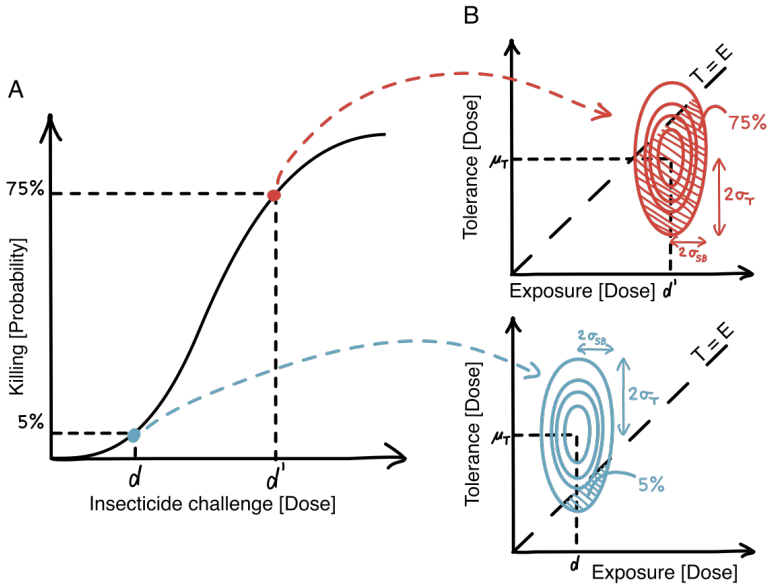

Fig 2. Our mechanistic model for insecticide-induced mosquito mortality in a ID-SB. A Illustration of the modelled relation between the insecticide dose tested in a ID-SB ('insecticide challenge') and the probability for killing a mosquito from a given population. **B** Illustration of how the killing probability is computed for a low dose d (blue) and high dose d' (red) used to challenge mosquitoes in a ID-SBs. The parameters μ_{T} and σ_{T} define the log-normal distribution of the insecticide tolerance in the mosquito population, and the challenged dose together with the parameter σ_{SB} define the log-normal distribution of the insecticide exposure in the SB. The joint distribution of exposure and tolerance take the form of a bivariate normal when plotted on the logarithmic scale, here displayed as contour lines. The killing probability for a given insecticide challenge is given by the probability that the exposure exceeds the tolerance ($E > T$).

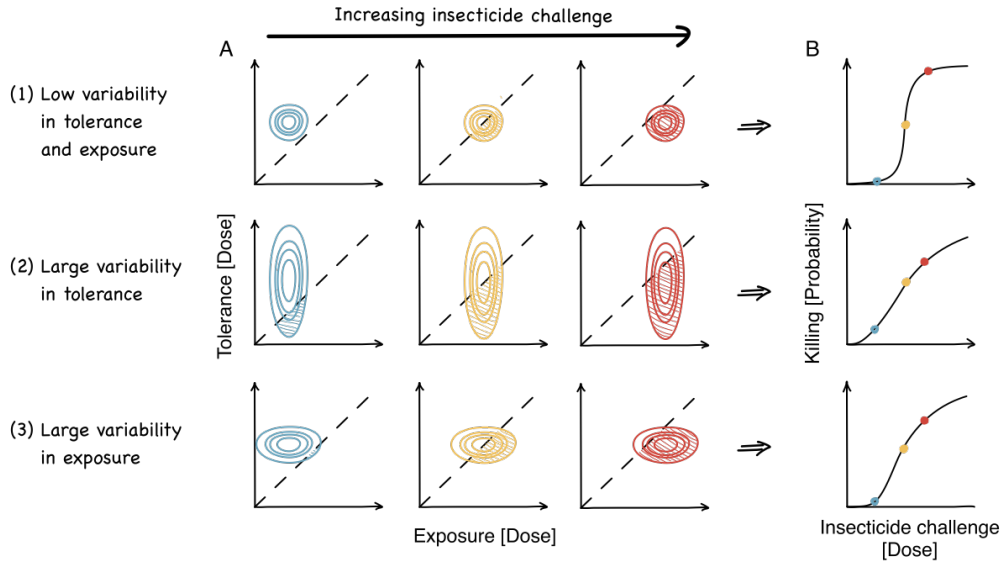

Fig 3. How variation in insecticide tolerance and exposure impact the dose-response relation under our mechanistic model. For the three scenarios of (1) low variability in both tolerance and exposure, (2) large variability in tolerance, and (3) large variability in exposure, we each display **A** the exposure-tolerance distribution for increasing insecticide challenge on the logarithmic scale, and **B** the corresponding dose-response curve of the mosquito killing probability for increasing insecticide challenge on the actual scale.

Similarly to Eq. 3, we assume an independent background mortality process with probability ${p^{(0)}}_{\text{EHT}}$ of death for a given EHT study. Again, the death of mosquito i is a Bernoulli random variable with probability

$$p_{\text{EHT}} = {p^{(0)}}_{\text{EHT}} + \left(1 - {p^{(0)}}_{\text{EHT}}\right) {p^{(1)}}_{\text{EHT}}. \tag{8}$$

Modelling the counts of dead mosquitoes in susceptibility bioassays and experimental hut trials

Assuming insecticide exposure and lethal dose are conditionally independent given the bioassay type and the resistance setting, respectively, the count of mosquitoes dying in a assay replicate follows a binomial distributions. So for each assay pair, j, corresponding to all SB and EHT data from a given village-sized geographical location and a given year (for details on matching SB and EHT studies see the Data section), we can derive the following sampling distributions. For the SBs, we have

$$D_{\text{SB}jk} \sim \text{binomial}\left(N_{\text{SB}jk}, p_{\text{SB}}\left({p^{(0)}}_{\text{SB}}, d_{jk}, \mu_{Tj}, \sigma_{Tj}, \sigma_{\text{SB}}\right)\right), \tag{9}$$

where $D_{\text{SB}jk}$ is the count of dead mosquitoes and $N_{\text{SB}jk}$ the total number of mosquitoes tested in the kth SB replicate of assay pair j. The probability of death p_{SB} in the corresponding SB replicate is a function of the insecticide dose d_{jk} applied in the SB replicate and the parameters described in Table 2, as defined in Eqs 3 and 5. For the corresponding EHT, we have

$$D_{\text{EHT}jl} \sim \text{binomial}\left(N_{\text{EHT}jl}, p_{\text{EHT}}\left({p^{(0)}}_{\text{EHT}}, \mu_{Tj}, \sigma_{Tj}, \mu_{\text{EHT}}, \sigma_{\text{EHT}}\right)\right), \tag{10}$$

where $D_{\mathrm{EHT}jl}$ is the count of dead mosquitoes and $N_{\mathrm{EHT}jl}$ the total number of mosquito captured in the hut in the lth EHT replicate of assay pair j. The death probability p_{EHT} in the corresponding EHT replicate is a function of the parameters described in Table 2, as defined by Eqs 7 and 8.

Taken together, the models defined in Eqs 9 and 10 form the joint model across different bioassays for a given resistance setting. The two sub-models are coupled via the common parameters $\mu_{\mathrm{T}j}$ and $\sigma_{\mathrm{T}j}$ per assay pair j, which completely define the lethal dose distribution for the corresponding resistance setting. The exposure parameters σ_{SB}, μ_{EHT}, and σ_{EHT} are fixed across all assay pairs. By coupling of the two sub-models (Eqs. 9 and 10), the exposure in EHTs is defined on the same scale – 'Dose' – as the exposure in the SBs. Although we estimated independent natural death probabilities in the EHTs for each assay pair j (${p^{(0)}}_{\mathrm{EHT}j}$), we assumed the same natural death probability in the SBs across all assay pairs (${p^{(0)}}_{\mathrm{SB}}$) since for the DD-SB studies there were no control data available. Assuming conditional independence across all assay pairs, we multiply the probabilities corresponding to Eqs. 9 and 10 to produce the sampling distribution for all data in Table 1 and S1 Table.

Predicting the killing effect of ITNs from intensity dose susceptibility bioassays

The objective of this study is to provide a calibrated model to predict the effectiveness of an ITN in killing mosquitoes in a given setting, as measured in an EHT, directly from ID-SBs with the corresponding insecticide in the same setting. After calibrating the parameters σ_{SB}, μ_{EHT} and σ_{EHT} of the joint model with the present data, the resistance characteristics $(\mu_{\mathrm{T}*}, \sigma_{\mathrm{T}*})$ of a previously unknown setting $*$ may be estimated from the new ID-SB data by the SB sub-model (Eq. 9). These estimates may then be plugged into the EHT sub-model (Eq. 10) to predict the killing effect of an ITN with the corresponding insecticide in a hypothetical EHT, as illustrated in S1 Fig for an example setting.

Bayesian inference

The joint model composed of the two sub-models (Eqs. 9 and 10) was fitted to the full data set (Table 1). In addition, the SB model (Eqs. 9) was fitted separately to the ID-SB data (Table 1) with independent natural death probabilities ${p^{(0)}}_{\mathrm{SB}j}$ per assay pair j. We fitted the models using a Bayesian framework, with prior distributions shown in Table 2. These were generally weakly informative (S2 Fig shows prior predictive checks) with the exception of the prior for the daily background mortality probability (i.e., mosquito mortality in the presence of no insecticide) which we assumed had 65% prior probability mass below 10% mortality.

Both models were fitted using the probabilistic language Stan [48] and the posteriors were sampled using Stan's default NUTS algorithm [49] accessed through the rstan package v2.26.1 [50] in R version 4.4.0 [51]. For the SB model and the joint model, we ran 4 chains with $4,000$ and $6,000$ iterations, respectively, and each time discarded half of the iterations as warm-up. To reduce the need for warm-up, we initialised the chains with point estimates obtained by optimisation; to obtain these point estimates, we used Stan's L-BFGS algorithm and used the set with the highest log-posterior across 10 optimisation runs. For processing the Stan output, we used the tidybayes R package [52]. For all model fits, we diagnosed convergence with $\hat{R} < 1.01$ and bulk- and tail-effective sample sizes above 400 for all model parameters [53]. For making statements about estimated quantities with a certain credibility, we relied on central credible intervals (i.e. equally tailed quantile intervals) for univariate quantities because

of their invariance with respect to monotonic transformations, and on highest density credible regions for multivariate quantities because of the lack of a natural choice for the quantile function for a multi-variate random variable.

Table 2. Summary of model parameters and prior distributions.

Parameter	Description	Prior distribution
μ_{T_j}	mean of log lethal dose in setting j	normal$(5, 10)$
σ_{T_j}	SD of log lethal dose in setting j	half-normal$(0, 5)$
σ_{SB}	SD of log insecticide exposure in SB	half-normal$(0, 5)$
μ_{EHT}	mean of log insecticide exposure in EHT	normal$(0, 5)$
σ_{EHT}	SD of log insecticide exposure in EHT	half-normal$(0, 5)$
${p^{(0)}}_{\mathrm{SB}}$	natural death probability in SB	beta$(1, 10)$
${p^{(0)}}_{\mathrm{EHT}_j}$	natural death probability in EHT for setting j	beta$(1, 10)$

Note that all parameters had independent prior distributions. SD means 'Standard deviation'.

Reproducibility

The data and code used to generate the presented results are publicly available [54]. The code is released under the MIT licence. Relevant software and packages are mentioned in the corresponding methods sections. All analyses were conducted in a Linux environment (Ubuntu 22.04.4). Inference with Hamiltonian Monte Carlo methods is inherently stochastic, and, while we fixed and reported the seeds for the random number generation, running the same code on another computing environment may lead to minorly different parameter estimates.

Results

The mechanistic model can integrate results from different bioassays

Fig 4 shows that the joint model (Eqs 9 and 10) fit simultaneously to all SB and EHT data recovered the mortality trends in both assays. Numerical summaries of the posterior predictive ITN killing effect in EHTs are contained in S2 Table. The model-based predictions are reasonable even for the studies with single-dose DD-SB for which the two-parameter resistance characterisation typically is not well identifiable (indicated by large posterior parameter correlation; see S2 Table). The predictions are generally a better fit for SB than for EHT studies, which was to be expected since, in the former experiment, conditions are more controlled. When the model-based predictions of EHT mortality are far from the observed mortality probability, the uncertainty of the latter is generally large (Fig 4). Inferred insecticide resistance characteristics and ITN killing effects for all assay pairs are shown in S3 Fig and summarised numerically in S2 Table; the inference for all parameters of the underlying model is summarised in S3 Table.

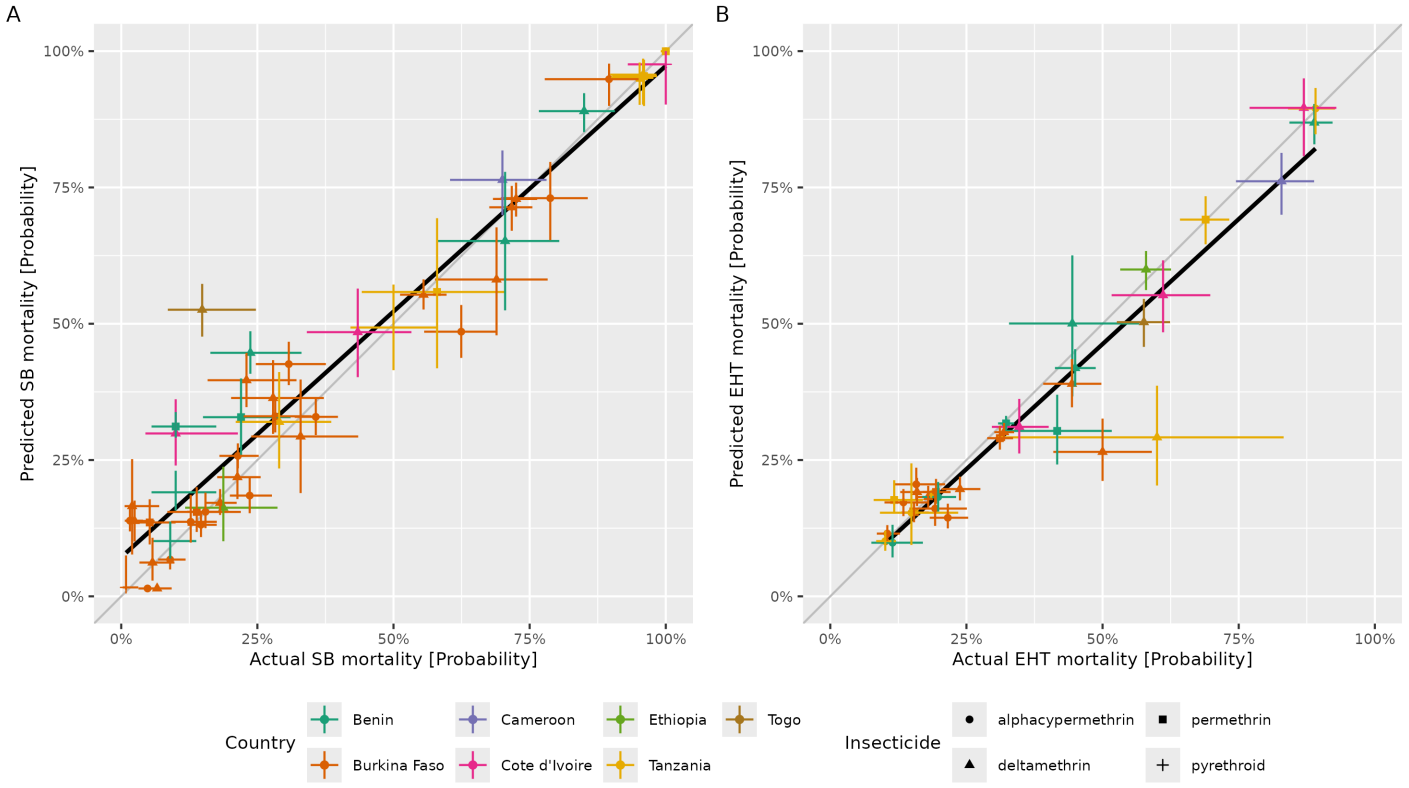

Fig 4. Model performance in susceptibility bioassays and experimental hut trials. Mortality in **A** susceptibility bioassays (SBs) and **B** experimental hut trials (EHTs), for 35 different assay pairs matched by geographical location, year and insecticide (see Table 1 for assay pair specification). For each assay pair, and each dose of the included intensity dose SBs, the mortality probability estimated by a binomial model with uniform prior probability ('actual') is plotted against the mortality probability estimated by the mechanistic model fitted to all SB and EHT data jointly ('predicted'). Point estimates correspond to the posterior median and interval estimates to 95% central, quantile-based credible intervals. A linear regression of the posterior medians (black) is plotted to visualise an actual versus predicted fit. The insecticide was recorded as 'pyrethroid' if different insecticides were pooled for the corresponding assay pair (see Data section and Table 1).

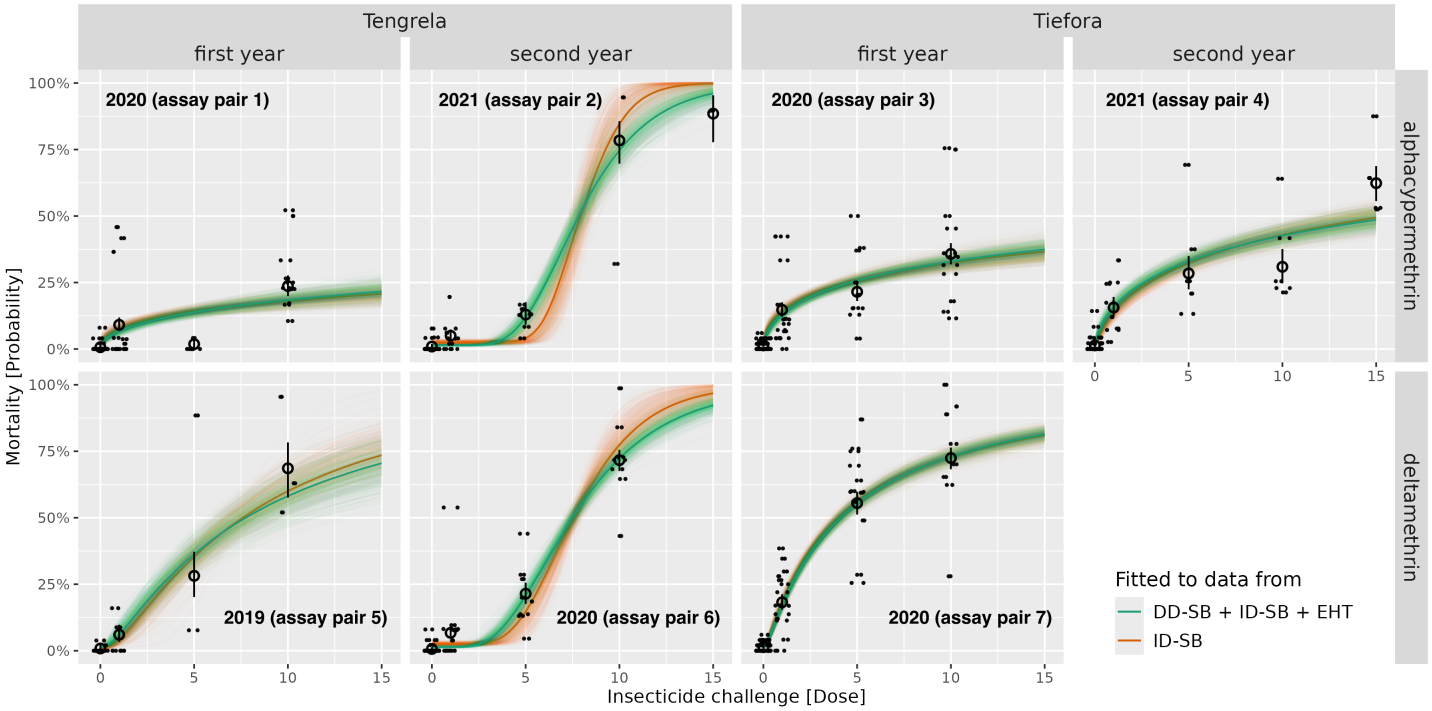

Fig 5. Model fits to intensity-dose susceptibility bioassay data from Burkina Faso. Each panel corresponds to one of the assay pairs which included intensity-dose susceptibility bioassay (ID-SB) data (see Table 1). Each panel reports the observed mortality percentages in the corresponding ID-SB replicates across the tested doses (black points, plotted with random jitter), the median mortality per dose (black circles), and the 95% central credible intervals of the mortality probability per dose as estimated with a separate binomial model per assay pair and dose (black vertical bars). 'Dose' refers to multiples of the discriminating dose defined by the WHO [35]. Note that for deltamethrin, doses 1, 5 and 10 were tested, and for alphacypermethrin there was an additional dose at 15. The underlaid dose-response curves correspond to the estimates of the mechanistic model for mortality in ID-SBs, either fitted simultaneously together with the experimental hut trial (EHT) model to all DD-SB and EHT data (green) or fitted separately only to ID-SB data (orange). The thick dose-response curves are the median posterior predictive model estimates with respect to the two fits; corresponding uncertainty is depicted by 500 curves that were generated with parameter sets sampled randomly from the corresponding posteriors. Summaries of the posteriors for all parameters underlying the two model estimates are contained in S3 Table and S4 Table.

Varied insecticide susceptibility dose-response patterns are captured by the mechanistic model

Our mechanistic model could represent the ID-SB data patterns from Burkina Faso which comprised two locations over three years and two insecticides, as shown by the estimated dose-response curves in Fig 5. However, for two resistance settings (assay pairs 1 and 4), the model estimates did not align well with the data since our mechanistic model only supports S-shaped dose-response curves. In addition to the joint model fit to all data, we fitted the SB model (Eq. 9) to the ID-SB data only (see S4 Table for parameter inference). By comparing the dose-response curves across the two fits (Fig 5), we showed that the resistance metrics, which uniquely define the curves, are inferred from the ID-SB data with only minimal influence by the EHT data in the joint model fit. This is important since, in the future, we want to predict the ITN killing probability in a hypothetical EHT from ID-SB data only by use of the joint model with exposure parameters calibrated by the present study.

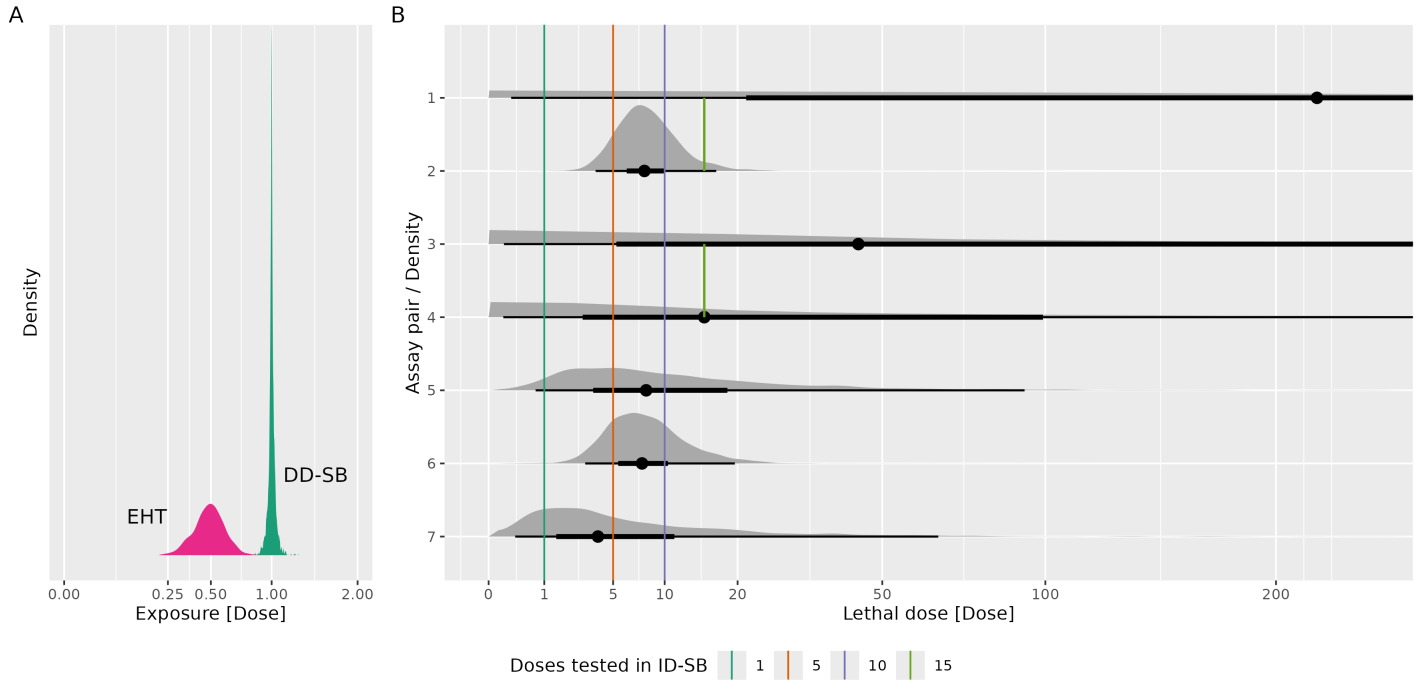

Fig 6. The estimated exposure in susceptibility bioassays and experimental hut trials, and the estimated insecticide tolerance across resistance settings. A Posterior predictive distributions of the exposure to pyrethroid insecticides in susceptibility bioassays (SBs) and experimental hut trials (EHTs) on the 'Dose' scale (multiples of the discriminating dose defined by the WHO [35]), as estimated by the joint mechanistic model. We assumed the same variance of the log-exposure distribution across discriminating-dose SBs (DD-SBs) and intensity-dose SBs (ID-SBs), so that the depicted DD-SB exposure distribution (green) represents the exposure variability across all considered SBs. For ID-SBs, the log-exposure distribution is shifted to be centred at the corresponding dose, with equal variance. The horizontal axis is on the square root scale. **B** Posterior predictive lethal dose distributions across all resistance settings with ID-SB data (assay pairs 1-7, see Tab. 1). Grey areas depict densities, black points denote medians and black lines show central, quantile-based credible intervals for probability levels of 50% and 95%. Vertical lines indicate the doses – which equal the median exposure in the ID-SB – against which the insecticide tolerance was tested in each ID-SB. The horizontal axis is on the square root scale. To facilitate the density estimation for this plot, we removed the top 0.05% percentile of the sampling points.

Quantifying differences in insecticide exposure across assays

Our mechanistic model allows for a comparison of insecticide exposure in SBs compared to EHTs. The estimated exposure distributions in Fig 6A indicate that exposure in EHTs was markedly lower and more variable than in SBs. In particular, the median exposure in EHTs was 0.49 $[0.38, 0.60]$ (posterior median and 95% credible interval) times the discriminating dose defined by the WHO, and the standard deviation of the exposure measured on the logarithmic scale was 0.14 $[0.02, 0.28]$ in EHTs compared to 0.02 $[0.00, 0.07]$ in SBs.

Improved characterisation of resistance using estimates of tolerance heterogeneity

We characterise the resistance of a local mosquito population against a given insecticide by the heterogeneity of insecticide tolerance in the population in addition to the median lethal dose. This two-parameter resistance metric allows for a more detailed comparison

of resistance profiles across different locations, years, and pyrethroid types. Fig 7A graphically displays the estimated resistance characteristics for the assay pairs comprising ID-SBs, including uncertainty quantification (highest density credible regions). The two parameters could be inferred from ID-SB data, but estimates were highly correlated if the insecticide challenge didn't explore the full mortality range (assay pairs 1, 3 and 4, see S2 Table). Fig 6B shows the corresponding lethal dose distributions, which are markedly more dispersed for the assay pairs 1, 3, and 4 compared to the others, due to the higher heterogeneity in insecticide tolerance and the more uncertain median lethal dose estimates. The resistance characteristics for the assay pairs that comprise only DD-SBs are depicted in S3 Fig A and summarised numerically in S2 Table, but these estimates were typically highly correlated and uncertain.

There was no consistent inter-location difference in resistance characteristics for the two villages Tengrela and Tiefora in Burkina Faso. With respect to intra-location resistance dynamics, we estimated that in Tengrela tolerance heterogeneity against both insecticides decreased over time (assay pairs 1 versus 2 for alphacypermethrin and 5 versus 6 for deltamethrin). We estimated that the lethal dose distribution was considerably wider for alphacypermethrin compared to deltamethrin in both locations (assay pairs 1 versus 6 for Tengrela and 3 versus 7 for Tiefora). Across both locations and both insecticides, we found that the lethal dose was well beyond the insecticide exposure in an EHT for most mosquitoes (compare the lethal dose distributions in Fig 6B to the EHT exposure distribution in Fig 6A), and the ITN killing effects were therefore very low (Fig 7B).

Predicting ITN killing effects across resistance settings with different characteristics

In Fig 7 we predict the ITN killing effect for a range of possible resistance characteristics, given the calibrated joint model (median posterior predictive killing probability). As expected, the ITN killing effect decreases with increasing median lethal dose (LD_{50}), with a decrease rate depending on the tolerance heterogeneity measure (σ_T) (Fig 7 C.1 and C.2). Regardless of the σ_T value, a 50% ITN killing effect is achieved if the median lethal dose is the same as the median exposure in the EHT. Varying the tolerance heterogeneity measure (σ_T) shows a more nuanced effect on EHT mortality (Fig 7 D.1 and D.2): Low heterogeneity (small σ_T values) accentuate extremes in the ITN killing effect for low and high μ_T. High heterogeneity (large σ_T values) pushes the ITN killing effect towards 50% since it produces highly dispersed lethal dose distributions.

Discussion

We presented a mechanistic model of insecticide-induced mosquito mortality in bioassays that explicitly describes the interaction of mosquitoes with the insecticide. By fitting the model to data from a range of malarial locations in Sub-Saharan Africa, we have illustrated that the model provides a common framework for interpreting and comparing data from a range of phenotypic insecticide bioassays. Namely, we proposed a two-parameter resistance metric, given by the median lethal dose and a measure of heterogeneity in insecticide tolerance, for improved characterisation of resistance profiles across sites. Generally, the larger the heterogeneity measure, the more robust the ITN killing effect with respect to variation of the insecticide exposure, for example, due to differences in housing structures.

EHTs are thought to provide a realistic emulation of the performance of ITNs in the field, and a direct outcome of them is a measure of the killing effect of ITNs. Our model provides a framework for using data collected from considerably cheaper ID-SBs to

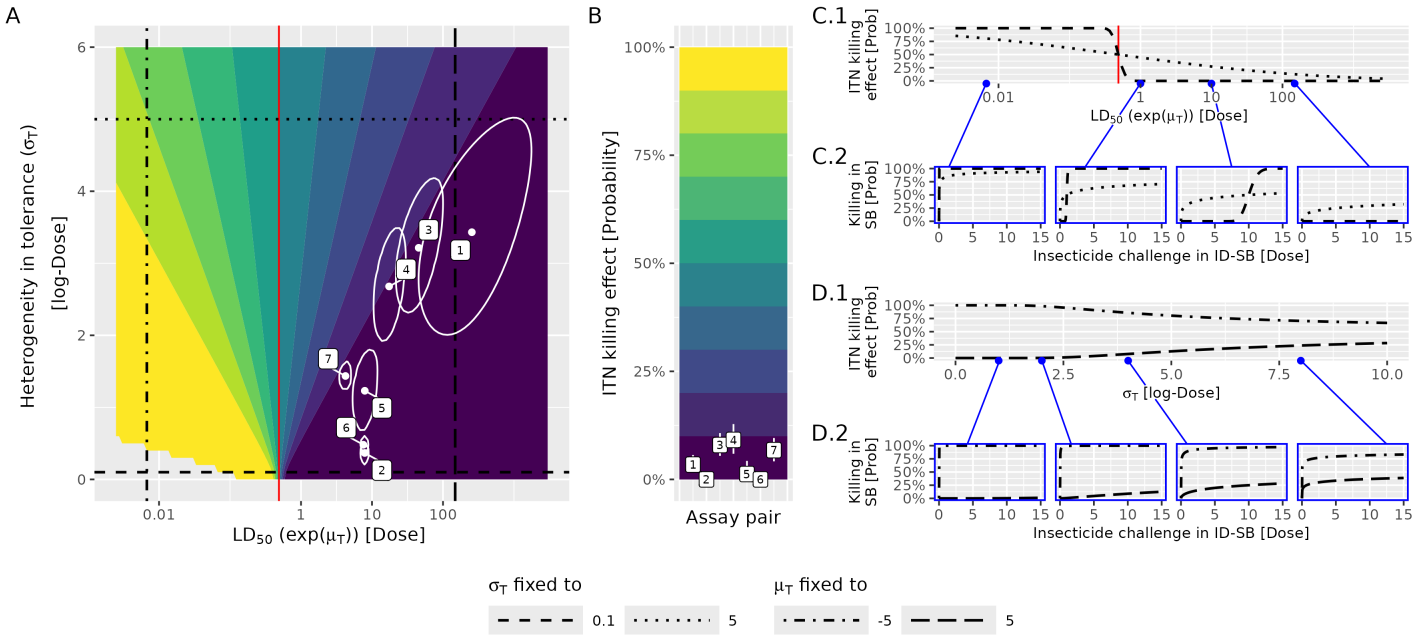

Fig 7. Estimated insecticide resistance characterisation and ITN killing effect. A Insecticide resistance characterisations by the median lethal dose (LD_{50}, equal to $\exp(\mu_T)$) and the proposed tolerance heterogeneity measure (standard deviation of the logarithm of the lethal dose, σ_T) for all assay pairs which comprised intensity-dose susceptibility bioassays (ID-SB) (assay pairs 1–7, see Table 1). Labelled dots (white) represent posterior medians, and curves (white) encompass 95% highest density credible regions. Numerical summaries of the estimated resistance characteristics are contained in S2 Table. Coloured areas correspond to binned posterior predictive ITN killing probabilities (posterior median, see panel B for colour legend), as estimated by the joint mechanistic model. The red vertical line marks the estimated median insecticide exposure in an EHT (posterior median). Black horizontal lines represent transects through the parameter space at σ_T values of 0.1 and 5, and black vertical lines transects at LD_{50} values of 0.007 and 148.4 (μ_T values of -5 and 5, respectively), with corresponding ITN killing effects and ID-SB dose-response curves displayed in panels C and D. **B** Posterior predictive ITN killing probabilities corresponding to the resistance settings characterised in A (assay pairs 1-7, see Table 1), displayed by the posterior median (square white markers) and central, quantile-based 95% credible intervals (vertical white lines). Numerical summaries of the estimated ITN killing probabilities are contained in S2 Table. **C.1** Posterior predictive ITN killing effect when varying the median lethal dose (LD_{50}) while fixing the tolerance heterogeneity (σ_T) to either 0.1 or 5 (dashed and dotted curve, respectively, corresponding to the horizontal transects in panel A). The red vertical line marks the estimated median insecticide exposure in EHT (posterior median). **C.2** Corresponding example dose-response curves for selected LD_{50} values of 0.007, 1, 10 and 148.4 (corresponding to μ_T values of $-5, 0, \log(10)$ and 5, respectively). **D.1** Posterior predictive ITN killing effects when varying the tolerance heterogeneity (σ_T), while fixing the median lethal dose (LD_{50}) to either 0.007 ($\mu_T = -5$) or 148.4 ($\mu_T = 5$) (dot-dashed and long-dashed curve, respectively, corresponding to the vertical transects in panel A). **D.2** Corresponding example dose-response curves for selected σ_T values of $1, 2, 4$ and 8. 'Dose' refers to multiples of the discriminating dose defined by the WHO [35].

emulate the results of a hypothetical EHT. Our estimated ITN killing effects for the assay pairs comprising ID-SB data were, however, consistently low, which reflects high levels of resistance in the relatively few studies where both ID-SB and EHT data were available. Our model needs to be reassessed once data from a more diverse range of sites become available. This will allow exploration of the levels of exposure observed in EHTs with different structural designs to allow more reliable comparisons of different products and mosquito populations between sites.

Previously, non-mechanistic models have been used to infer a heuristic link between mortality in DD-SBs and EHTs [13, 28], and these estimates were subject to large uncertainty. In response to the need for new resistance testing guidelines to better inform control programmes [55], ID-SBs were developed [39] and the dose-mortality relationship has been analysed using flexible statistical models [40]. Our characterisation of resistance is similar to the lethal concentration estimated in [40], but the approaches differ in the underlying model. In [40], the lethal concentration distribution is defined by fitting a flexible sigmoidal curve (a generalised logistic function of five parameters) to the ID-SB data and interpreting that curve as the cumulative distribution function of the lethal concentration. This means that the shape of the dose-response curve is entirely reflected by the lethal concentration distribution, implicitly assuming identical exposure of all mosquitoes. In contrast, we allow for stochastic exposure and, under some distributional assumptions, we derive a cumulative distribution function for mortality. This means that the shape of our dose-responses curve is described by both the variance of the lethal dose and the exposure in the mosquito population, while the dose where the curve reaches 50% mortality is entirely determined by the median lethal dose. Despite its mathematical simplicity, our model fits the ID-SB data well relative to these more heuristic statistical approaches, and its mechanistic nature provides greater interpretability.

We do not explicitly account for non-experimentally controllable factors of the killing effect of ITNs in EHTs. Factors that were present during the matched SB study, such as mosquito species composition and microbe infections in the local mosquito population, are implicitly accounted for when predicting ITN killing effects from SB data. In contrast, factors that varied between the SB and ETH studies of a matched assay pair – such as environmental conditions (including during the juvenile mosquito stages) and very localised conditions at the EHT site, such as sugar feeding opportunities – are missed and may contribute to poor predictive performance. Furthermore, we currently treat data from two different years from the same geographic location as two independent entomological settings. Future work with a larger and richer data set is needed to further investigate the sources of variation in biossay results.

For the calibration of the exposure parameters, we fitted a joint model simultaneously to the SB and EHT data. This is problematic since the resistance characterisation parameters are likely informed by both the SB and the EHT data, while they must be inferred from the SB data alone when making predictions of ITN effectiveness for settings without EHT data. Moreover, the EHT model is likely less well specified due to less controlled experimental conditions and may affect the inference of the SB model parameters. The undesirable feedback of information in the inference could be prevented by using the *cut* approach [56] instead of a joint modelling approach. However, we still opt for the joint modelling approach due to the computational burden and the conceptual difficulties of a fully Bayesian interpretation of the cut posterior [57, 58]. Additionally, joint inference appears reasonable for our data set since we confirmed that fitting the SB model to ID-SB data separately results in almost identical dose-response curves (Fig 5).

In further research, we plan to use the proposed resistance characterisation to better quantify the effectiveness of ITNs over their useful life by taking into account the decay

of insecticide concentrations [59]. A possible correlation between insecticide susceptibility and insecticide exposure of individual mosquitoes could be readily accounted for in our model, but the present data do not allow us to identify the needed correlation coefficient. Video tracking data of mosquito-net interaction in cone assays [44] and EHT [45] could be used to estimate this correlation and, by so doing, probe and isolate the impact of behavioural resistance.

Our mechanistic model, with exposure parameters calibrated by the present study, can predict the ITN killing effect for locations without EHTs but where cheaper and increasingly used ID-SB studies are conducted. This would enable wider-scale calibration of transmission models to local insecticide resistance profiles. This is an important step towards refining the recommendations for ITN deployment strategies in the presence of resistance to pyrethroids [9] in order to improve the epidemiological benefit of these important global health tools.

Acknowledgements

We thank all the researchers who made the data available for inclusion in this study.

Funding

Research reported in this publication was supported by personal fellowships to Adrian Denz (Swiss National Science Foundation, SNSF, Grant Numbers 203017, 225815), Antoine Sanou (Wellcome Trust, 222019/Z/20/Z) and project grants from the National Institute of Allergy and Infectious Diseases of the National Institutes of Health (Award Number R01AI116811) and the Bill & Melinda Gates Foundation (OPP1200155). Thomas S. Churcher acknowledges funding from the Medical Research Council (MRC) Centre for Global Infectious Disease Analysis (Reference Number MR/R015600/1), jointly funded by the MRC and the UK Foreign, Commonwealth and Development Office (FCDO), under the MRC/FCDO Concordat agreement, and is also part of the EDCTP2 programme supported by the European Union. The content is solely the responsibility of the authors and does not necessarily represent the official views of the National Institutes of Health or other funders.

Supporting information

S1 Fig. Identifying the parameters that characterise a given resistance setting and predicting the corresponding ITN killing effect with the proposed mechanistic model A Example killing probabilities for different doses (vertical lines) tested in an intensity-dose susceptibility bioassay (ID-SB) with assumed example dose-response relation (black curve). 'Dose' refers to multiples of the discriminating dose defined by the WHO [35]. **B** Contour lines for example killing probabilities (see panel A) in the parameter space characterising the resistance setting. The two-parameter resistance characterisation (black circle), which completely defines the dose-response curve (see panel A), is identifiable if the ID-SB explored the full mortality range across the given doses. **C** Estimated resistance characterisation (white dot) and binned ITN killing probabilities across the parameters space characterising possible resistance characterisations for example parameters of insecticide exposure in EHTs. The parameters of insecticide exposure in EHTs (μ_{EHT} and σ_{EHT}, see Table 2) are identifiable if the data set comprises a sufficient range of ITN killing probabilities. **D** Estimated ITN killing probability for the given example. For this example resistance setting, we arbitrarily choose a median lethal dose of 2.23 ($\mu_{\mathrm{T}} = 0.8$) and a tolerance

heterogeneity measure (standard deviation of the logarithm of the lethal dose, σ_{T}) of 1. For exposure in SB and EHT assays, we arbitrarily choose the parameter values $\sigma_{\mathrm{SB}} = 0.2$, $\mu_{\mathrm{EHT}} = 1.0$ and $\sigma_{\mathrm{EHT}} = 0.5$ (see Table 2 for a description of those parameters).

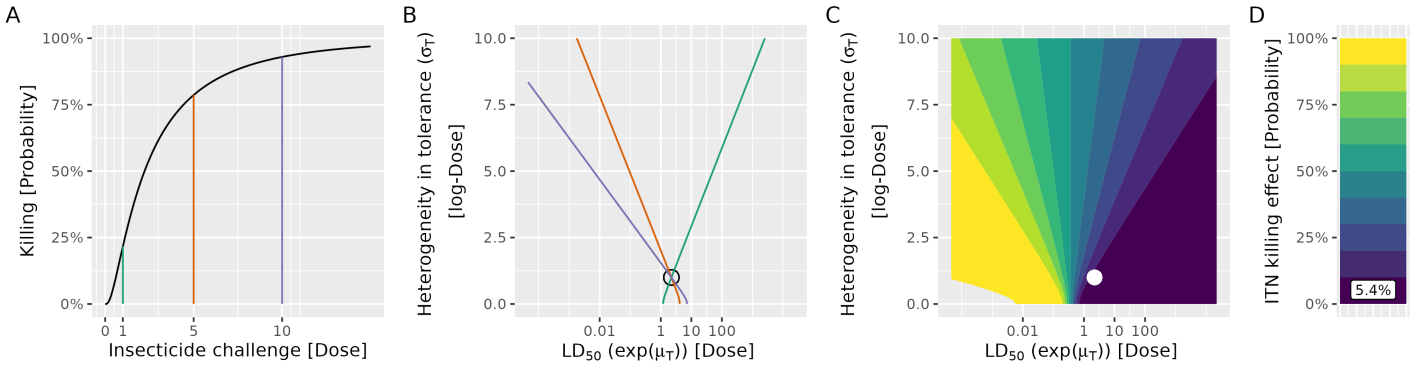

S2 Fig. Prior predictive checks. Mortality in **A** intensity-dose susceptibility bioassays (ID-SB; on the logarithmic scale), **B** discriminating-dose susceptibility bioassays (DD-SB) and **C** experimental hut trials (EHT) under the respective mechanistic models with parameters sampled from the priors (see Table 2). For the ID-SB model, the specified priors support a wide variety of dose-response curves (fine blue curves). The prior predictive mortalities for control SB and DD-SB are identical to those of the corresponding doses in ID-SB.

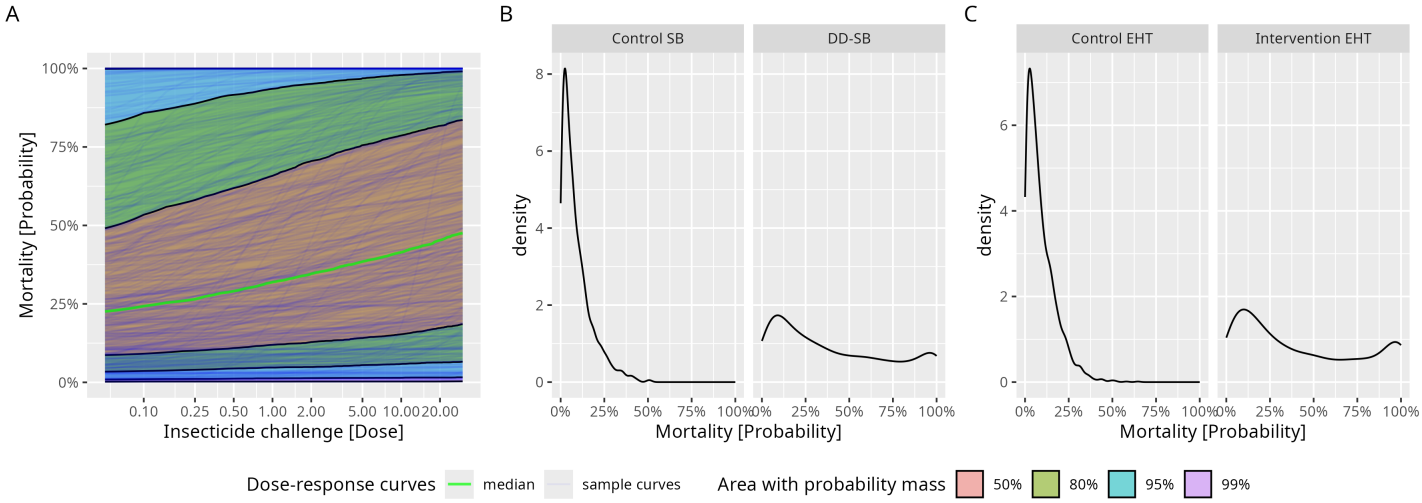

S3 Fig. Estimated insecticide resistance characterisation and ITN killing effect. A Characterisations of insecticide resistance by median lethal dose and proposed measure of heterogeneity in insecticide tolerance (standard deviation of the logarithm of the lethal dose, σ_{T}) for all assay pairs (see Table 1 for assay pair specification), displayed by the posterior median (white dots). Note that the uncertainty may be very

large and the posterior correlation between μ_T and σ_T very strong for assay pairs with only DD-SB data (see S2 Table). The coloured areas display binned posterior predictive ITN killing probabilities (posterior median; see panel B for the colour legend) for a range of insecticide resistance characterisations, as estimated by the joint mechanistic model. The red vertical line marks the estimated median insecticide exposure in an EHT (posterior median). **B** Posterior predictive ITN killing probabilities for all assay pairs (see Table 1 for assay pair specification), displayed as posterior median (square white markers) and quantile-based 95% credible intervals (vertical white lines).

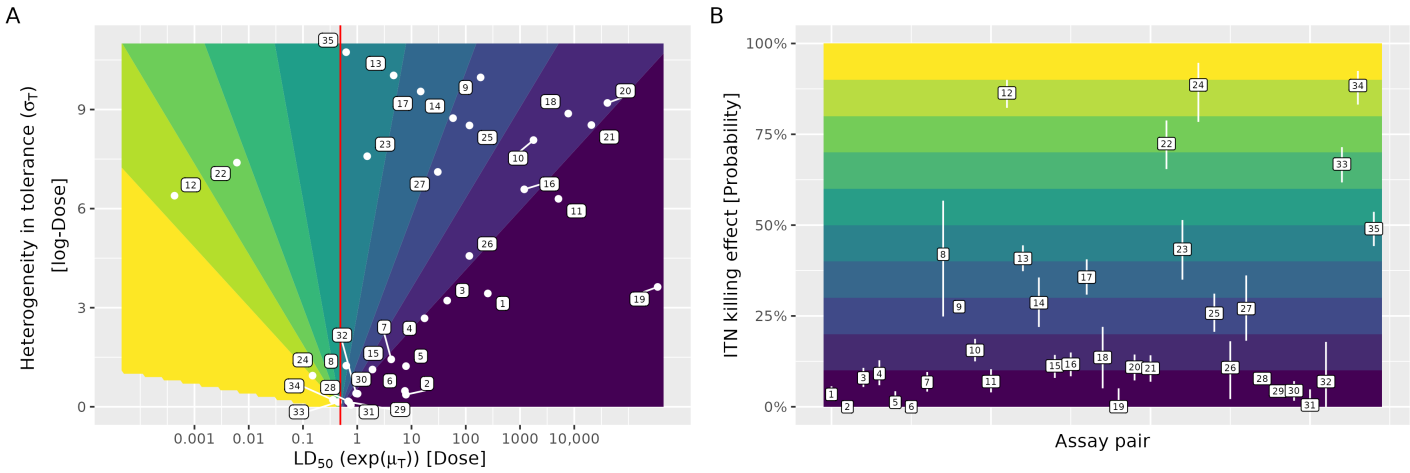

S1 Table. Summary of paired DD-SB and EHT data used in this study.

Assay pair	Reference	Country	Site	Year	SB protocol	Hut type	Insecticides in SB	Insecticides on ITNs	ITN products	Total in treatment SB	Total in control SB	Total in intervention hut	Total in control hut
8	[60]	Benin	Akron	2010	WHO	West	deltamethrin	deltamethrin	LifeNet	61	0	63	144
9	[61]	Benin	Cove	2010	WHO	West	permethrin	permethrin	Olyset	100	0	3804	2874
10	[62]	Benin	Cove	2012	WHO	West	deltamethrin, permethrin	alphacypermethrin	Interceptor	100	0	631	673
11	[63]	Benin	Cove	2015	WHO	West	deltamethrin, permethrin	alphacypermethrin	Interceptor	200	0	175	310
12	[64]	Benin	Malanville	2008	WHO	West	deltamethrin	deltamethrin	PermaNet2	100	0	243	285
13	[60]	Benin	Malanville	2010	WHO	West	deltamethrin	deltamethrin	LifeNet	97	0	676	911
14	[65]	Benin	Malanville	2011	WHO	West	permethrin	permethrin	Olyset	100	0	96	69
15	[66]	Burkina Faso	Tengrela	2014	WHO	West	deltamethrin	deltamethrin	DawaPlus2, PermaNet2	85	0	1485	482
16	[66]	Burkina Faso	Tengrela	2014	WHO	West	permethrin	permethrin	Olyset	101	0	922	482
17	[64]	Burkina Faso	VDK	2007	WHO	West	deltamethrin	deltamethrin	PermaNet2	100	0	329	908
18	[67]	Burkina Faso	VDK	2011	WHO	West	deltamethrin	deltamethrin	PermaNet2	100	0	114	336
19	[68]	Burkina Faso	VDK	2014	WHO	West	deltamethrin, permethrin	alphacypermethrin	Interceptor	227	0	519	853
20	[66]	Burkina Faso	VK5	2014	WHO	West	deltamethrin	deltamethrin	DawaPlus2, PermaNet2	163	0	2532	1095
21	[66]	Burkina Faso	VK5	2014	WHO	West	permethrin	permethrin	Olyset	153	0	1458	1095
22	[64]	Cameroon	Pitoa	2008	WHO	West	deltamethrin	deltamethrin	PermaNet2	100	0	105	401
23	[69]	Cote d'Ivoire	Tiassale	2012	WHO	West	deltamethrin	deltamethrin	PermaNet2	99	0	108	130
24	[70]	Cote d'Ivoire	Yaokoffikro	2000	pre2000	West	pyrethroid	deltamethrin	PermaNet	50	0	69	84
25	[71]	Cote d'Ivoire	Yaokoffikro	2009	WHO	West	deltamethrin	deltamethrin	PermaNet2	50	0	317	796
26	[72]	Ethiopia	GGDam	2011	WHO	East	deltamethrin	deltamethrin	PermaNet2	80	0	426	511
27	[73]	Tanzania	LowerMoshi	2013	WHO	East	deltamethrin	deltamethrin	PermaNet2	100	0	10	75
28	[74]	Tanzania	Lupiro	2010	WHO	Ifakara	deltamethrin	deltamethrin	PermaNet2, Icon Life	96	0	30431	11777
29	[74]	Tanzania	Lupiro	2010	WHO	Ifakara	permethrin	permethrin	Olyset	125	0	15836	11777
30	[75]	Tanzania	Lupiro	2015	WHO	Ifakara	deltamethrin, lambdacyhalothrin, permethrin	alphacypermethrin	MAGNet	150	0	1070	810
31	[76]	Tanzania	Mabogini	2005	WHO	East	permethrin	permethrin	Olyset	100	0	196	716
32	[75]	Tanzania	Muheza	2015	WHO	East	permethrin	alphacypermethrin	Interceptor	50	0	94	139
33	[77]	Tanzania	Zeneti	2005	WHO	East	permethrin	permethrin	Olyset	393	0	399	854
34	[78]	Tanzania	Zeneti	2006	WHO	East	alphacypermethrin	alphacypermethrin	Interceptor	752	0	202	252
35	[79]	Togo	Kolokope	2013	WHO	West	deltamethrin	deltamethrin	Yorkool	74	0	389	465

S1 Table. Summary of the paired DD-SB and EHT data used in this study. Note that controls may be shared between assay pairs. For a summary of the paired

ID-SB and EHT data used in this study see Table 1.

S2 Table. Model predictions per assay pair from the joint SB and EHT model Point estimates (median) and interval estimates (quantile-based 95% credible intervals) for the estimated ITN killing effect, the median lethal dose (LD_{50}) and the standard deviation of the logarithm of the lethal dose (σ_T) as a measure of heterogeneity in insecticide tolerance, as estimated from the joint SB and EHT model. The Pearson correlation coefficient ($\mathrm{Cor}(\mu_T, \sigma_T)$) between the mean ($\mu_T$) and the standard deviation (σ_T) of the logarithm of the lethal dose indicates how well the resistance characterisation by these two parameters could be identified from the data. The closer 0 is, the better the characterisation could be identified.

S3 Table. Parameter estimates and sampling diagnostics from the joint SB and EHT model Mean, median, standard deviation (SD), median absolute deviation (MAD), 5% Quantile, 95% Quantile, a MCMC convergence diagnostic (Rhat), bulk effective sample size (ESS_bulk) and tail effective sample size (ESS_tail) for all posterior parameter samples of the joint model for SB and EHT data. For explanations on MCMC inference diagnostics, see [53].

S4 Table. Parameter estimates and sampling diagnostics from the SB only model Mean, median, standard deviation (SD), median absolute deviation (MAD), 5% Quantile, 95% Quantile, a MCMC convergence diagnostic (Rhat), bulk effective sample size (ESS_bulk) and tail effective sample size (ESS_tail) for all posterior parameter samples of the model for SB data only. For explanations on MCMC inference diagnostics, see [53].

References

1. Organization WH. World Malaria Report 2023; 2023.
2. Magesa SM, Wilkes TJ, Mnzava AEP, Njunwa KJ, Myamba J, Kivuyo MDP, et al. Trial of Pyrethroid Impregnated Bednets in an Area of Tanzania Holoendemic for Malaria Part 2. Effects on the Malaria Vector Population. Acta Tropica. 1991;49(2):97–108. doi:10.1016/0001-706X(91)90057-Q.
3. Hawley WA, Phillips-Howard PA, Kuile FOT, Terlouw DJ, Vulule JM, Ombok M, et al. COMMUNITY-WIDE EFFECTS OF PERMETHRIN-TREATED BED NETS ON CHILD MORTALITY AND MALARIA MORBIDITY IN WESTERN KENYA. The American Journal of Tropical Medicine and Hygiene. 2003;68(4_suppl):121–127. doi:10.4269/ajtmh.2003.68.121.
4. Killeen GF, Smith TA, Ferguson HM, Mshinda H, Abdulla S, Lengeler C, et al. Preventing Childhood Malaria in Africa by Protecting Adults from Mosquitoes with Insecticide-Treated Nets. PLOS Medicine. 2007;4(7):e229. doi:10.1371/journal.pmed.0040229.
5. Chitnis N, Schapira A, Smith T, Steketee R. Comparing the Effectiveness of Malaria Vector-Control Interventions Through a Mathematical Model. The American Journal of Tropical Medicine and Hygiene. 2010;83(2):230–240. doi:10.4269/ajtmh.2010.09-0179.
6. Birget PLG, Koella JC. An Epidemiological Model of the Effects of Insecticide-Treated Bed Nets on Malaria Transmission. PLOS ONE. 2015;10(12):e0144173. doi:10.1371/journal.pone.0144173.

7. Unwin HJT, Sherrard-Smith E, Churcher TS, Ghani AC. Quantifying the Direct and Indirect Protection Provided by Insecticide Treated Bed Nets against Malaria. Nature Communications. 2023;14:676. doi:10.1038/s41467-023-36356-9.

8. Bhatt S, Weiss DJ, Cameron E, Bisanzio D, Mappin B, Dalrymple U, et al. The Effect of Malaria Control on Plasmodium Falciparum in Africa between 2000 and 2015. Nature. 2015;526(7572):207–211. doi:10.1038/nature15535.

9. Organization WH. WHO | Global Plan for Insecticide Resistance Management in Malaria Vectors; 2012.

10. Hemingway J. The Role of Vector Control in Stopping the Transmission of Malaria: Threats and Opportunities. Philosophical Transactions of the Royal Society B: Biological Sciences. 2014;369(1645):20130431. doi:10.1098/rstb.2013.0431.

11. Thomas MB, Read AF. The Threat (or Not) of Insecticide Resistance for Malaria Control. Proceedings of the National Academy of Sciences. 2016;113(32):8900–8902. doi:10.1073/pnas.1609889113.

12. Ranson H, Lissenden N. Insecticide Resistance in African Anopheles Mosquitoes: A Worsening Situation That Needs Urgent Action to Maintain Malaria Control. Trends in Parasitology. 2016;32(3):187–196. doi:10.1016/j.pt.2015.11.010.

13. Churcher TS, Lissenden N, Griffin JT, Worrall E, Ranson H. The Impact of Pyrethroid Resistance on the Efficacy and Effectiveness of Bednets for Malaria Control in Africa. eLife. 2016;5:e16090. doi:10.7554/eLife.16090.

14. Hemingway J, Ranson H, Magill A, Kolaczinski J, Fornadel C, Gimnig J, et al. Averting a Malaria Disaster: Will Insecticide Resistance Derail Malaria Control? The Lancet. 2016;387(10029):1785–1788. doi:10.1016/S0140-6736(15)00417-1.

15. Hemingway J. The Way Forward for Vector Control. Science. 2017;358(6366):998–999. doi:10.1126/science.aaj1644.

16. Ranson H. Current and Future Prospects for Preventing Malaria Transmission via the Use of Insecticides. Cold Spring Harbor Perspectives in Medicine. 2017;7(11):a026823. doi:10.1101/cshperspect.a026823.

17. Kleinschmidt I, Bradley J, Knox TB, Mnzava AP, Kafy HT, Mbogo C, et al. Implications of Insecticide Resistance for Malaria Vector Control with Long-Lasting Insecticidal Nets: A WHO-coordinated, Prospective, International, Observational Cohort Study. The Lancet Infectious Diseases. 2018;18(6):640–649. doi:10.1016/S1473-3099(18)30172-5.

18. Organization WH. Manual for Monitoring Insecticide Resistance in Mosquito Vectors and Selecting Appropriate Interventions; 2022.

19. Kleinschmidt I, Mnzava AP, Kafy HT, Mbogo C, Bashir AI, Bigoga J, et al. Design of a Study to Determine the Impact of Insecticide Resistance on Malaria Vector Control: A Multi-Country Investigation. Malaria Journal. 2015;14(1):282. doi:10.1186/s12936-015-0782-4.

20. Lindsay SW, Thomas MB, Kleinschmidt I. Threats to the Effectiveness of Insecticide-Treated Bednets for Malaria Control: Thinking beyond Insecticide Resistance. The Lancet Global Health. 2021;9(9):e1325–e1331. doi:10.1016/S2214-109X(21)00216-3.

21. Smith T, Killeen GF, Maire N, Ross A, Molineaux L, Tediosi F, et al. Mathematical Modeling of the Impact of Malaria Vaccines on the Clinical Epidemiology and Natural History of Plasmodium Falciparum Malaria: Overview. The American journal of tropical medicine and hygiene. 2006;75(2 suppl):1–10.

22. Griffin JT, Hollingsworth TD, Okell LC, Churcher TS, White M, Hinsley W, et al. Reducing Plasmodium Falciparum Malaria Transmission in Africa: A Model-Based Evaluation of Intervention Strategies. PLOS Medicine. 2010;7(8):e1000324. doi:10.1371/journal.pmed.1000324.

23. Eckhoff PA. A Malaria Transmission-Directed Model of Mosquito Life Cycle and Ecology. Malaria Journal. 2011;10:303. doi:10.1186/1475-2875-10-303.

24. Sherrard-Smith E, Winskill P, Hamlet A, Ngufor C, N'Guessan R, Guelbeogo MW, et al. Optimising the Deployment of Vector Control Tools against Malaria: A Data-Informed Modelling Study. The Lancet Planetary Health. 2022;6(2):e100–e109. doi:10.1016/S2542-5196(21)00296-5.

25. Yadav R, WHOPES. Guidelines for Laboratory and Field Testing of Long-Lasting Insecticidal Nets. WHO. 2013; p. vii, 89.

26. Killeen GF, Kihonda J, Lyimo E, Oketch FR, Kotas ME, Mathenge E, et al. Quantifying Behavioural Interactions between Humans and Mosquitoes: Evaluating the Protective Efficacy of Insecticidal Nets against Malaria Transmission in Rural Tanzania. BMC Infectious Diseases. 2006;6(1):161. doi:10.1186/1471-2334-6-161.

27. Briët OJ, Penny MA, Hardy D, Awolola TS, Van Bortel W, Corbel V, et al. Effects of Pyrethroid Resistance on the Cost Effectiveness of a Mass Distribution of Long-Lasting Insecticidal Nets: A Modelling Study. Malaria Journal. 2013;12(1):77. doi:10.1186/1475-2875-12-77.

28. Nash RK, Lambert B, N'Guessan R, Ngufor C, Rowland M, Oxborough R, et al. Systematic Review of the Entomological Impact of Insecticide-Treated Nets Evaluated Using Experimental Hut Trials in Africa. Current Research in Parasitology & Vector-Borne Diseases. 2021;1:100047. doi:10.1016/j.crpvbd.2021.100047.

29. Smith A. A Verandah-Trap Hut for Studying the House-Frequenting Habits of Mosquitos and for Assessing Insecticides. I.—A Description of the Verandah-Trap Hut and of Studies on the Egress of Anopheles Gambiae Giles and Mansonia Uniformis (Theo.) from an Untreated Hut. Bulletin of Entomological Research. 1965;56(1):161–167. doi:10.1017/S0007485300057114.

30. Darriet F, N'Guessan R, Hougard JM, Traoré-Lamizana M, Carnevale P. [An experimental tool essential for the evaluation of insecticides: the testing huts]. Bulletin De La Societe De Pathologie Exotique (1990). 2002;95(4):299–303.

31. Okumu FO, Moore J, Mbeyela E, Sherlock M, Sangusangu R, Ligamba G, et al. A Modified Experimental Hut Design for Studying Responses of Disease-Transmitting Mosquitoes to Indoor Interventions: The Ifakara Experimental Huts. PLOS ONE. 2012;7(2):e30967. doi:10.1371/journal.pone.0030967.

32. Massue DJ, Kisinza WN, Malongo BB, Mgaya CS, Bradley J, Moore JD, et al. Comparative Performance of Three Experimental Hut Designs for Measuring Malaria Vector Responses to Insecticides in Tanzania. Malaria Journal. 2016;15(1):165. doi:10.1186/s12936-016-1221-x.

33. Moyes CL, Wiebe A, Gleave K, Trett A, Hancock PA, Padonou GG, et al. Analysis-Ready Datasets for Insecticide Resistance Phenotype and Genotype Frequency in African Malaria Vectors. Scientific Data. 2019;6(1):121. doi:10.1038/s41597-019-0134-2.

34. Organization WH. Malaria Threat Map; 2024. https://apps.who.int/malaria/maps/threats/#/stories?theme=prevention.

35. Organization WH. Test Procedures for Insecticide Resistance Monitoring in Malaria Vector Mosquitoes. 2nd ed. World Health Organization; 2016.

36. Centers for Disease Control and Prevention (U S). CONUS Manual for Evaluating Insecticide Resistance in Mosquitoes Using the CDC Bottle Bioassay Kit; 2022.

37. Sherrard-Smith E, Ngufor C, Sanou A, Guelbeogo MW, N'Guessan R, Elobolobo E, et al. Inferring the Epidemiological Benefit of Indoor Vector Control Interventions against Malaria from Mosquito Data. Nature Communications. 2022;13(1):3862. doi:10.1038/s41467-022-30700-1.

38. Bagi J, Grisales N, Corkill R, Morgan JC, N'Falé S, Brogdon WG, et al. When a Discriminating Dose Assay Is Not Enough: Measuring the Intensity of Insecticide Resistance in Malaria Vectors. Malaria Journal. 2015;14(1):210. doi:10.1186/s12936-015-0721-4.

39. Corbel V, Kont MD, Ahumada ML, Andréo L, Bayili B, Bayili K, et al. A New WHO Bottle Bioassay Method to Assess the Susceptibility of Mosquito Vectors to Public Health Insecticides: Results from a WHO-coordinated Multi-Centre Study. Parasites & Vectors. 2023;16:21. doi:10.1186/s13071-022-05554-7.

40. Kont MD, Lambert B, Sanou A, Williams J, Ranson H, Foster GM, et al. Characterising the Intensity of Insecticide Resistance: A Novel Framework for Analysis of Intensity Bioassay Data. Current Research in Parasitology & Vector-Borne Diseases. 2023;4:100125. doi:10.1016/j.crpvbd.2023.100125.

41. Challenger JD, Nash RK, Ngufor C, Sanou A, Toé KH, Moore S, et al. Assessing the Variability in Experimental Hut Trials Evaluating Insecticide-Treated Nets against Malaria Vectors. Current Research in Parasitology & Vector-Borne Diseases. 2023;3:100115. doi:10.1016/j.crpvbd.2023.100115.

42. Moyes CL, Lees RS, Yunta C, Walker KJ, Hemmings K, Oladepo F, et al. Assessing Cross-Resistance within the Pyrethroids in Terms of Their Interactions with Key Cytochrome P450 Enzymes and Resistance in Vector Populations. Parasites & Vectors. 2021;14(1):115. doi:10.1186/s13071-021-04609-5.

43. Sanou A. Personal Communication; 2024.

44. Jones J, Matope A, Barreaux P, Gleave K, Steen K, Ranson H, et al. Video Augmentation of the WHO Cone Assay to Quantify Mosquito Behavioural Responses to Insecticide-Treated Nets. Parasites & Vectors. 2023;16(1):420. doi:10.1186/s13071-023-06029-z.

45. Angarita-Jaimes NC, Parker JEA, Abe M, Mashauri F, Martine J, Towers CE, et al. A Novel Video-Tracking System to Quantify the Behaviour of Nocturnal Mosquitoes Attacking Human Hosts in the Field. Journal of The Royal Society Interface. 2016;13(117):20150974. doi:10.1098/rsif.2015.0974.

46. Hancock PA, Ochomo E, Messenger LA. Genetic Surveillance of Insecticide Resistance in African Anopheles Populations to Inform Malaria Vector Control. Trends in Parasitology. 2024;40(7):604–618. doi:10.1016/j.pt.2024.04.016.

47. Hobbs NP, Weetman D, Hastings IM. Insecticide Resistance Management Strategies for Public Health Control of Mosquitoes Exhibiting Polygenic Resistance: A Comparison of Sequences, Rotations, and Mixtures. Evolutionary Applications. 2023;16(4):936–959. doi:10.1111/eva.13546.

48. StanDevelopmentTeam. Stan Modeling Language Users Guide and Reference Manual, v2.34; 2024.

49. Hoffman MD, Gelman A. The No-U-Turn Sampler: Adaptively Setting Path Lengths in Hamiltonian Monte Carlo. Journal of Machine Learning Research. 2014;.

50. Stan Development Team. RStan: The R Interface to Stan; 2023.

51. R Core Team. R: A Language and Environment for Statistical Computing; 2024. R Foundation for Statistical Computing.

52. Kay M, Mastny T. Tidybayes: Tidy Data and 'Geoms' for Bayesian Models; 2024.

53. Vehtari A, Gelman A, Simpson D, Carpenter B, Bürkner PC. Rank-Normalization, Folding, and Localization: An Improved Rˆ for Assessing Convergence of MCMC (with Discussion). Bayesian Analysis. 2021;16(2):667–718. doi:10.1214/20-BA1221.

54. Denz A. SB2EHT_mech; 2025. https://github.com/a-e-e-m/SB2EHT_mech.

55. Namias A, Jobe NB, Paaijmans KP, Huijben S. The Need for Practical Insecticide-Resistance Guidelines to Effectively Inform Mosquito-Borne Disease Control Programs. eLife. 2021;10:e65655. doi:10.7554/eLife.65655.

56. Plummer M. Cuts in Bayesian Graphical Models. Statistics and Computing. 2015;25(1):37–43. doi:10.1007/s11222-014-9503-z.

57. Jacob PE, Murray LM, Holmes CC, Robert CP. Better Together? Statistical Learning in Models Made of Modules; 2017.

58. Liu Y, Goudie RJB. A General Framework for Cutting Feedback within Modularized Bayesian Inference; 2022.

59. Briet O, Koenker H, Norris L, Wiegand R, Vanden Eng J, Thackeray A, et al. Attrition, Physical Integrity and Insecticidal Activity of Long-Lasting Insecticidal Nets in Sub-Saharan Africa and Modelling of Their Impact on Vectorial Capacity. Malaria Journal. 2020;19(1):310. doi:10.1186/s12936-020-03383-6.

60. Agossa FR, Padonou GG, Gnanguenon V, Oké-Agbo F, Zola-Sahossi J, Dègnonvi H, et al. Laboratory and Field Evaluation of the Impact of Washings on the Effectiveness of LifeNet®, Olyset® and PermaNet® 2.0 in Two Areas, Where There Is a High Level of Resistance of Anopheles Gambiae to Pyrethroids, Benin, West Africa. Malaria Journal. 2014;13(1):193. doi:10.1186/1475-2875-13-193.

61. Ngufor C, N'Guessan R, Fagbohoun J, Todjinou D, Odjo A, Malone D, et al. Efficacy of the Olyset Duo Net against Insecticide-Resistant Mosquito Vectors of Malaria. Science Translational Medicine. 2016;8(356):356ra121–356ra121. doi:10.1126/scitranslmed.aad3270.

62. N'Guessan R, Odjo A, Ngufor C, Malone D, Rowland M. A Chlorfenapyr Mixture Net Interceptor® G2 Shows High Efficacy and Wash Durability against Resistant Mosquitoes in West Africa. PLOS ONE. 2016;11(11):e0165925. doi:10.1371/journal.pone.0165925.

63. Ngufor C, Fagbohoun J, Critchley J, N'Guessan R, Todjinou D, Malone D, et al. Which Intervention Is Better for Malaria Vector Control: Insecticide Mixture Long-Lasting Insecticidal Nets or Standard Pyrethroid Nets Combined with Indoor Residual Spraying? Malaria Journal. 2017;16(1):340. doi:10.1186/s12936-017-1987-5.

64. Corbel V, Chabi J, Dabiré RK, Etang J, Nwane P, Pigeon O, et al. Field Efficacy of a New Mosaic Long-Lasting Mosquito Net (PermaNet® 3.0) against Pyrethroid-Resistant Malaria Vectors: A Multi Centre Study in Western and Central Africa. Malaria Journal. 2010;9:113. doi:10.1186/1475-2875-9-113.

65. Pennetier C, Bouraima A, Chandre F, Piameu M, Etang J, Rossignol M, et al. Efficacy of Olyset® Plus, a New Long-Lasting Insecticidal Net Incorporating Permethrin and Piperonil-Butoxide against Multi-Resistant Malaria Vectors. PLOS ONE. 2013;8(10):e75134. doi:10.1371/journal.pone.0075134.

66. Toe KH, Müller P, Badolo A, Traore A, Sagnon N, Dabiré RK, et al. Do Bednets Including Piperonyl Butoxide Offer Additional Protection against Populations of Anopheles Gambiae s.l. That Are Highly Resistant to Pyrethroids? An Experimental Hut Evaluation in Burkina Fasov. Medical and Veterinary Entomology. 2018;32(4):407–416. doi:10.1111/mve.12316.

67. Ngufor C, Tchicaya E, Koudou B, N'Fale S, Dabire R, Johnson P, et al. Combining Organophosphate Treated Wall Linings and Long-lasting Insecticidal Nets for Improved Control of Pyrethroid Resistant Anopheles Gambiae. PLOS ONE. 2014;9(1):e83897. doi:10.1371/journal.pone.0083897.

68. Bayili K, N'do S, Namountougou M, Sanou R, Ouattara A, Dabiré RK, et al. Evaluation of Efficacy of Interceptor® G2, a Long-Lasting Insecticide Net Coated with a Mixture of Chlorfenapyr and Alpha-Cypermethrin, against Pyrethroid Resistant Anopheles Gambiae s.l. in Burkina Faso. Malaria Journal. 2017;16(1):190. doi:10.1186/s12936-017-1846-4.

69. Ngufor C, Chouaïbou M, Tchicaya E, Loukou B, Kesse N, N'Guessan R, et al. Combining Organophosphate-Treated Wall Linings and Long-Lasting Insecticidal Nets Fails to Provide Additional Control over Long-Lasting Insecticidal Nets Alone against Multiple Insecticide-Resistant Anopheles Gambiae in Côte d'Ivoire: An Experimental Hut Trial. Malaria Journal. 2014;13(1):396. doi:10.1186/1475-2875-13-396.

70. Guillet P, N'Guessan R, Darriet F, Traore-Lamizana M, Chandre F, Carnevale P. Combined Pyrethroid and Carbamate 'Two-in-One' Treated Mosquito Nets: Field Efficacy against Pyrethroid-Resistant Anopheles Gambiae and Culex Quinquefasciatus. Medical and Veterinary Entomology. 2001;15(1):105–112. doi:10.1046/j.1365-2915.2001.00288.x.

71. Koudou BG, Koffi AA, Malone D, Hemingway J. Efficacy of PermaNet® 2.0 and PermaNet® 3.0 against Insecticide-Resistant Anopheles Gambiae in Experimental Huts in Côte d'Ivoire. Malaria Journal. 2011;10(1):172. doi:10.1186/1475-2875-10-172.

72. Asale A, Getachew Y, Hailesilassie W, Speybroeck N, Duchateau L, Yewhalaw D. Evaluation of the Efficacy of DDT Indoor Residual Spraying and Long-Lasting Insecticidal Nets against Insecticide Resistant Populations of Anopheles Arabiensis Patton (Diptera: Culicidae) from Ethiopia Using Experimental Huts. Parasites & Vectors. 2014;7(1):131. doi:10.1186/1756-3305-7-131.

73. Kweka EJ, Lyaruu LJ, Mahande AM. Efficacy of PermaNet® 3.0 and PermaNet® 2.0 Nets against Laboratory-Reared and Wild Anopheles Gambiae Sensu Lato Populations in Northern Tanzania. Infectious Diseases of Poverty. 2017;6(1):11. doi:10.1186/s40249-016-0220-z.

74. Okumu FO, Mbeyela E, Lingamba G, Moore J, Ntamatungiro AJ, Kavishe DR, et al. Comparative Field Evaluation of Combinations of Long-Lasting Insecticide Treated Nets and Indoor Residual Spraying, Relative to Either Method Alone, for Malaria Prevention in an Area Where the Main Vector Is Anopheles Arabiensis. Parasites & Vectors. 2013;6(1):46. doi:10.1186/1756-3305-6-46.

75. Organization WH. Report of the Nineteenth WHOPES Working Group Meeting: Review of Veeralin LN, VectoMax GR, Bactivec SC. Geneva; 2016.

76. Mosha FW, Lyimo IN, Oxborough RM, Matowo J, Malima R, Feston E, et al. Comparative Efficacies of Permethrin-, Deltamethrin- and α -Cypermethrin-Treated Nets, against *Anopheles Arabiensis* and *Culex Quinquefasciatus* in Northern Tanzania. Annals of Tropical Medicine & Parasitology. 2008;102(4):367–376. doi:10.1179/136485908X278829.

77. Malima RC, Magesa SM, Tungu PK, Mwingira V, Magogo FS, Sudi W, et al. An Experimental Hut Evaluation of Olyset® Nets against Anopheline Mosquitoes after Seven Years Use in Tanzanian Villages. Malaria Journal. 2008;7(1):38. doi:10.1186/1475-2875-7-38.

78. Malima R, Tungu PK, Mwingira V, Maxwell C, Magesa SM, Kaur H, et al. Evaluation of the Long-Lasting Insecticidal Net Interceptor LN: Laboratory and Experimental Hut Studies against Anopheline and Culicine Mosquitoes in Northeastern Tanzania. Parasites & Vectors. 2013;6(1):296. doi:10.1186/1756-3305-6-296.

79. Ketoh GK, Ahadji-Dabla KM, Chabi J, Amoudji AD, Apetogbo GY, Awokou F, et al. Efficacy of Two PBO Long Lasting Insecticidal Nets against Natural Populations of Anopheles Gambiae s.l. in Experimental Huts, Kolokopé, Togo. PLOS ONE. 2018;13(7):e0192492. doi:10.1371/journal.pone.0192492.